

## FIRST RESULTS FROM THE FAINT OBJECT CAMERA: HIGH-RESOLUTION OBSERVATIONS OF THE CENTRAL OBJECT R136 IN THE 30 DORADUS NEBULA<sup>1</sup>

G. WEIGELT,<sup>2,3</sup> R. ALBRECHT,<sup>2,4,5</sup> C. BARBIERI,<sup>2,6</sup> J. C. BLADES,<sup>2,7</sup> A. BOKSEBERG,<sup>2,8</sup> P. CRANE,<sup>2,9</sup>  
 J. M. DEHARVENG,<sup>2,10</sup> M. J. DISNEY,<sup>2,11</sup> P. JAKOBSEN,<sup>2,12</sup> T. M. KAMPERMAN,<sup>2,13</sup>  
 I. R. KING,<sup>2,14</sup> F. MACCHETTO,<sup>2,5,7</sup> C. D. MACKAY,<sup>2,15</sup> F. PARESCE,<sup>2,5,7</sup>  
 D. BAXTER,<sup>7</sup> P. GREENFIELD,<sup>7</sup> R. JEDRZEJEWSKI,<sup>7</sup> A. NOTA,<sup>6,7</sup>  
 AND W. B. SPARKS<sup>7</sup>

Received 1991 April 15; accepted 1991 June 17

### ABSTRACT

R136 is the luminous central object of the giant H II region 30 Doradus in the Large Magellanic Cloud. We report on the first high-resolution observations of R136 with the Faint Object Camera on board the Hubble Space Telescope. The physical nature of the brightest component R136a has been a matter of some controversy over the last few years. The UV images obtained show that R136a is a very compact star cluster consisting of more than eight stars within 0".7 diameter. From these high-resolution images a mass upper limit can be derived for the most luminous stars observed in R136.

*Subject headings:* nebulae: H II regions — stars: binaries — stars: massive

### 1. INTRODUCTION

The 30 Doradus nebula is the dominant giant H II region in the Large Magellanic Cloud. At the center of 30 Doradus is a spectacular ionizing star cluster which contains many hot and very massive O and WR stars. Many of the O stars are of type O3, which are the most massive stars known. The central core of this cluster is the very luminous object R136 (Walborn 1973, 1984, 1986, 1990 and references therein; Feitzinger et al. 1980; Moffat & Seggewiss 1983; Chu & Wolfire 1983; Walker & O'Donoghue 1984; Weigelt & Baier 1985; Moffat, Seggewiss, & Shara 1985; Melnick 1985; Walborn & Blades 1987). The central object R136 (HD 38268) consists of the bright component R136a and the two fainter components b and c. R136a contributes about one-third of the ionization of the 30 Doradus nebula (Walborn 1986). The giant H II region 30

Doradus and its central object R136 are key objects for the understanding of similar starburst regions in more distant galaxies.

The physical nature of R136 has been the subject of controversy over the last few years. One suggestion was that R136a might be a single supermassive object with a mass of the order of 1000 solar masses. The other suggestion was that R136a is the dense core of the star cluster and that R136a consists of several O and WR stars (see review articles Walborn 1984, 1986, 1990). Observations of R136a by speckle techniques have shown that R136a consists of at least eight stars within 0".7 diameter (Weigelt & Baier 1985; Neri & Grewing 1988).

In this *Letter* we report the first observations of R136 with the HST Faint Object Camera (Macchetto et al. 1980; Macchetto 1982; Paresce 1990). The observations described in this *Letter* belong to a series of observations made to assess the quality of the data that can be obtained in spite of the spherical aberration of the HST (see Burrows et al. 1991). The R136 observations at UV wavelengths described here show that R136a is a very compact star cluster. There is good agreement with the speckle observations mentioned above. From the observations an upper limit for the most massive stars resolved in R136a can be derived.

### 2. OBSERVATIONS, DATA PROCESSING AND DISCUSSION

The observations reported in this paper are FOC observations in two different filters. The raw image shown in Figure 1 (Plate L1) was taken on 1990 August 23 with the filters F346M (central wavelength 3450 Å, bandwidth 432 Å) and F8ND (8 mag neutral density filter) in the f/96 mode. This image is an acquisition image taken with an exposure time of 600 s. Only the inner 11" × 11" region of the whole 22" × 22" exposure is shown. Since too many neutral density filters were used, the count number (number of detected photons) in the brightest pixel is only 136, corresponding to a count rate of ~0.23 counts pixel<sup>-1</sup> s<sup>-1</sup> in the brightest pixel. The optimum count rate would be 1 to 2 counts pixel<sup>-1</sup> s<sup>-1</sup>. The stars are slightly elongated since the telescope was tracking in coarse track mode. The diffuse background in the vicinity of the star cluster

<sup>1</sup> Based on observations with the NASA/ESA *Hubble Space Telescope*, obtained at the Space Telescope Science Institute, which is operated by AURA, Inc., under NASA contract NAS 5-26555.

<sup>2</sup> Member FOC Investigation Definition Team.

<sup>3</sup> Max-Planck-Institut für Radioastronomie, Auf dem Hügel 69, D-5300 Bonn 1, Germany.

<sup>4</sup> Space Telescope European Coordinating Facility, European Southern Observatory, Karl-Schwarzschild-Strasse 2, D-8046 Garching, Germany.

<sup>5</sup> Astrophysics Division, Space Science Department of ESA.

<sup>6</sup> Osservatorio Astronomico di Padova, Vicolo Osservatorio 5, I-35122 Padova, Italy (postal address for C. Barbieri).

<sup>7</sup> Space Telescope Science Institute, 3700 San Martin Drive, Baltimore, MD 21218.

<sup>8</sup> Royal Greenwich Observatory, Madingley Road, Cambridge CB3 0EZ, England, UK.

<sup>9</sup> European Southern Observatory, Karl-Schwarzschild-Strasse 2, D-8046 Garching, Germany.

<sup>10</sup> Laboratoire d'Astronomie Spatiale du CNRS, Traverse du Siphon, Les Trois Lucs, F-13012 Marseille, France.

<sup>11</sup> Department of Physics, University College of Cardiff, P.O. Box 713, Cardiff CF1 3TH, Wales, UK.

<sup>12</sup> Astrophysics Division, Space Science Department of ESA, ESTEC, NL-2200 AG Noordwijk, The Netherlands.

<sup>13</sup> SRON, Space Research Utrecht, Sorbonnelaan 2, NL-3584 CA Utrecht, The Netherlands.

<sup>14</sup> Astronomy Department, University of California, Berkeley, CA 94720.

<sup>15</sup> Institute of Astronomy, Madingley Road, Cambridge CB3 0HA, England, UK.



FIG. 1.—FOC f/96 raw image of R136 (filter F346M + F8ND)

WEIGELT et al. (see 378, L21)

is caused by the large wings of the telescope point spread function (see Burrows et al. 1991).

Figure 2 (Plate L2) shows the same R136 image after application of the image restoration method CLEAN (Högbom 1974), as discussed below in more detail. For image restoration a point spread function measured with an UV calibration star and the filter F346M was used.

The HST FOC exposure of R136 shown in Figure 3 (Plate L3) (raw image) was taken in the  $f/288$  mode (1990 August 23). The filters were F253M (central wavelength 2550 Å, bandwidth 232 Å), plus F4ND (4 mag neutral density filter). The exposure time was 900 s. The count number in the brightest pixel is only 27 due to an inappropriate selection of neutral density filters in these initial FOC observations.

Figure 4 shows the inner  $1''.7 \times 1''.7$  region of a high-resolution image of R136a reconstructed from the  $f/288$  raw image (Fig. 3) by the image restoration method CLEAN. This method is widely used in radio interferometry, especially for objects consisting of point sources. We also experimented with inverse and Wiener filtering. CLEAN worked better for R136 (but it worked worse than inverse or Wiener filtering in other experiments with diffuse extended objects). There are two main differences between HST data and radio interferometry data. (1) HST data are degraded by photon noise whereas radio data are degraded by other types of noise. (2) In radio interferometry data the point spread function (dirty beam) and the degraded image (dirty map) contain negative as well as positive sidelobes whereas in optical images the point spread function and the degraded image intensity are positive, of course. The CLEAN method used in our HST experiments was essentially Högbom's method (Högbom 1974). Before the application of CLEAN we convolved the raw image and the point spread function with a narrow Gaussian function ( $\sigma$  0.7 pixel). In each iteration of CLEAN the subtraction of a fraction of the point spread function was performed at the maximum positive value of the image (instead of maximum absolute value) since there were essentially no negative values. The absolute value of the

largest negative values was much less than 1% of the peak. The number of iterations was  $\sim 400$ , the loop gain was 0.1. The iteration process was stopped before noise spikes created false stars. The residuals were added to the restored component image. Normalization in the restored component image was done in such a way that flux conservation was obtained. The restored image was convolved with a low-pass filtered ideal point spread function. Because no point spread function was available for the F253M filter, it was necessary to improvise a point spread function. The closest available was F210M, taken at a closely neighboring but not identical focal position. This point spread function was used directly, and an alternative reconstruction was made with the size of the point spread function scaled by a suitable factor (this does not perfectly represent the point spread function, but it may well be closer to correctness). The two reconstructions did not differ appreciably; the discussion that follows refers to the scaled case.

In spite of the large amount of photon noise in the raw image, the resolution of the  $f/288$  reconstruction is higher than the  $f/96$  reconstruction. However, the photometric accuracy of the  $f/288$  reconstruction is not very good since the raw image is very noisy (27 counts in the brightest pixel). The reason for the good resolution is that the three times smaller pixels of the  $f/288$  mode (pixel size 7 mas) can better resolve the fine structure in the point spread function than the pixels of the  $f/96$  mode, as discussed in more detail by Müller & Weigelt (1987). The resolution of the  $f/288$  reconstruction is high enough to resolve the bright dominant quadruple star (a1, a2, a3, a6) including the close, bright  $0''.11$  double star (a1, a2). This object, which is reconstructed with high signal-to-noise ratio, is most important for the astrophysical discussions in the next sections.

In Table 1 the HST FOC  $f/288$  reconstruction and the image reconstructed by holographic speckle interferometry (Weigelt & Baier 1985) are compared. In the  $f/288$  raw image (filter F253M) the star R136a2 is  $\sim 0.4$  ( $\pm 0.2$ ) mag fainter than R136a1, while the stars R136a3 and R136a6 are  $\sim 0.6$  ( $\pm 0.3$ ) mag fainter than R136a1 (in Table 1 the same names as in the speckle paper are used). The accuracy of the relative magnitudes is rather low because of severe photon noise and the overlapping wings of the point spread functions. For the fainter stars it was not possible to derive magnitude differences because of the photon noise. The lowest contours in Figure 4 are very close to the noise level. Therefore, a few of the faintest stars may be spurious. In spite of the very different wavelengths, all eight stars resolved by holographic speckle interfer-

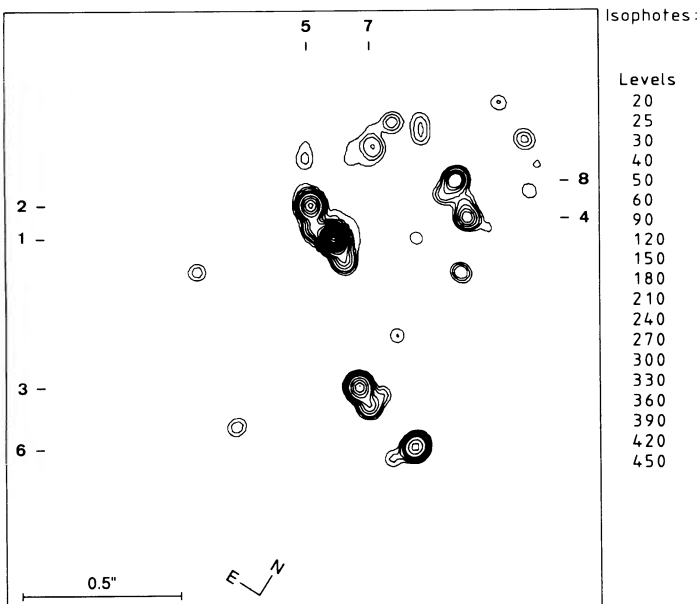


FIG. 4.—High-resolution image of R136a reconstructed from the FOC  $f/288$  image shown in Fig. 3.

TABLE 1  
SEPARATIONS AND POSITION ANGLES OF R136a STARS

R136	Speckle Observation (RG 610) Separation	FOC $f/288$ Observation (F253M) Separation	Speckle Observation (RG 610) Position Angle	FOC $f/288$ Observation (F253M) Position Angle
a1 .....	0'.00	0'.00	000°	000°
a2 .....	0.10	0.11	066	063
a3 .....	0.48	0.48	223	222
a4 .....	0.39	0.40	323	311
a5 .....	0.27	0.25	050	048
a6 .....	0.70	0.71	231	233
a7 .....	0.35	0.36	012	014
a8 .....	0.35	0.38	337	330



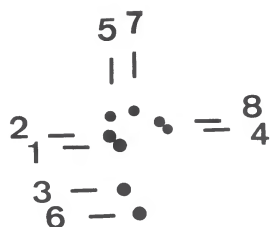


FIG. 2.—Image of R136 reconstructed from the FOC f/96 image shown in Fig. 1

WEIGELT et al. (see 378, L22)

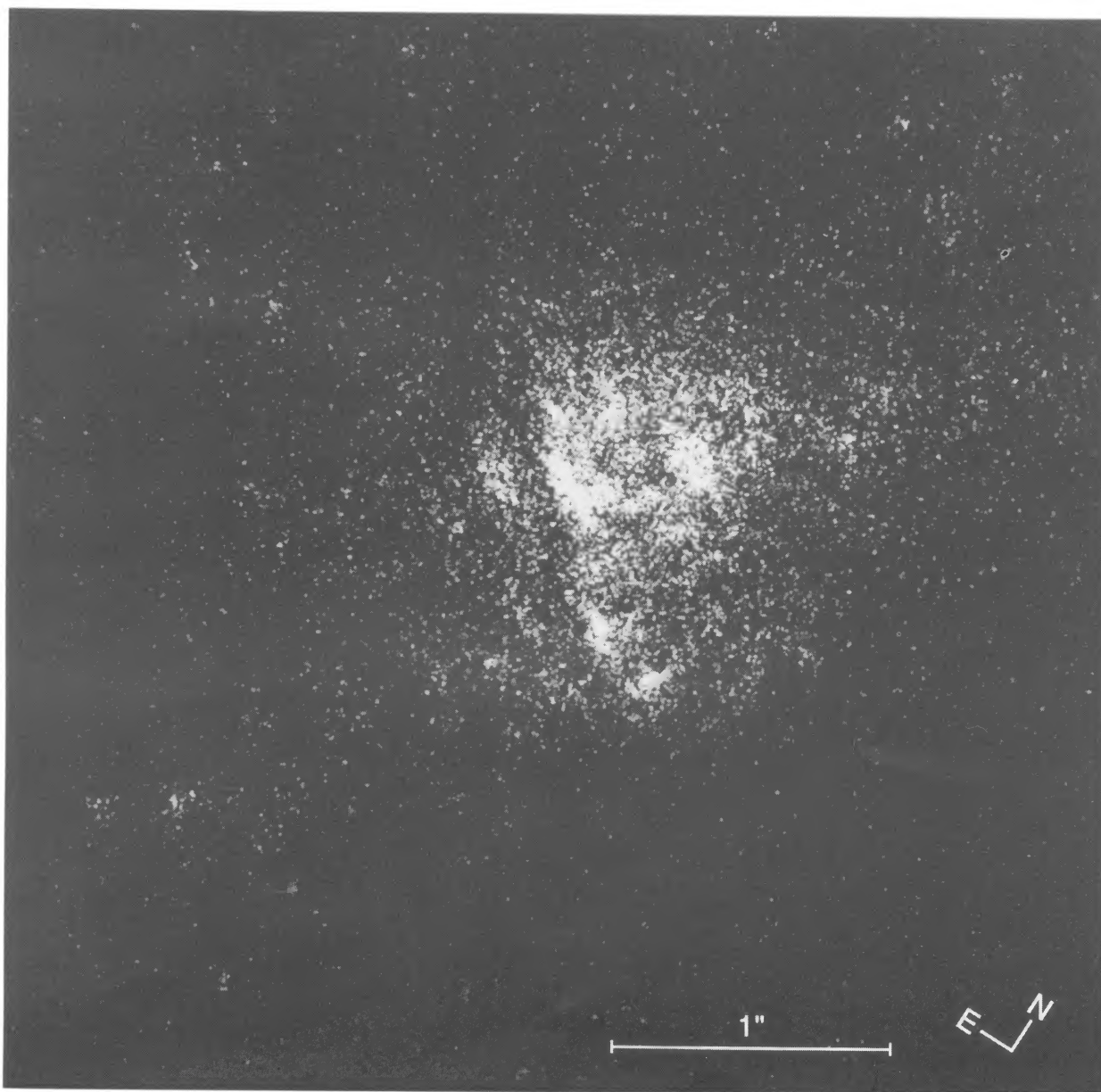


FIG. 3.—FOC  $f/288$  raw image of R136a (filter F253M + F4ND). The image looks very diffuse and noisy because of the large wings of the point spread function and because of the severe photon noise (27 counts in the brightest pixel).

WEIGELT et al. (see 378, L22)

ometry can be found in both the  $f/96$  and the  $f/288$  HST FOC images, including the close  $0''.11$  double star (a1, a2).

Walborn (1986) has calculated the mass of the brightest speckle component R136a1 on the assumption that the V-magnitudes of a2 and a3 are not more than  $\sim 0.3$  mag fainter than a1. In this case he finds an upper limit for the mass of R136a1 of  $\sim 250$  solar masses. From the speckle observations we know that in the red the magnitude differences are  $\sim 0-0.3$  (for a1, a2, and a3). From the HST observations we now know in addition that at  $2550 \text{ \AA}$  the magnitude differences are only  $\sim 0.4-0.6$  (for four stars). This means that the new HST observations support Walborn's assumptions and his conclusion that the upper limit for the mass of R136a1 is of the order of 250 solar masses. The brightest unresolved objects in R136 and

the surrounding cluster are the best current candidates for the most massive stars known.

The Faint Object Camera is the result of many years of hard work and important contributions by a number of highly dedicated individuals. In particular, we wish to thank ESA *HST* Project Manager Robin Laurance, the ESA/*HST* Project Team, and the European contractors for building an outstanding scientific instrument. The FOC IDT Support Team, D. B., P. G., R. J., and W. B. S. acknowledge support from ESA through contract 6500/85/NL/SK. P. C. and I. R. K. acknowledge support from NASA through contracts NAS5-27760 and NAS5-28086. Finally, we wish to thank N. Walborn for many helpful discussions.

## REFERENCES

- Burrows, C. J., Holtzman, J. A., Faber, S. M., Bely, P. Y., Hasan, H., Lynds, C. R., & Schroeder, D. 1991, *ApJ*, 369, L21  
 Chu, Y.-H., Cassinelli, J. P., & Wolfire, M. G. 1984, *ApJ*, 283, 560  
 Feitzinger, J. V., Schlosser, W., Schmidt-Kaler, Th., & Winkler, C. 1980, *A&A*, 84, 50  
 Högbom, J. 1974, *A&AS*, 15, 417  
 Macchetto, F. 1982, in *The Space Telescope Observatory, Special Session of Commission 44, IAU 18th General Assembly (Patras, Greece)*, ed. D. N. B. Hall (Washington: NASA Scientific and Technical Information Branch), NASA CP-2244, 40  
 Macchetto, F., van de Hulst, H. C., di Serego Alighieri, S., & Perryman, M. A. C. 1980, *The Faint Object Camera for the Space Telescope* (Noordwijk: ESTEC) ESA SP-1028  
 Melnick, J. 1985, *A&A*, 153, 235  
 Moffat, A. F. J., & Seggewiss, W. 1983, *A&A*, 125, 83  
 Moffat, A. F. J., Seggewiss, W., & Shara, M. M. 1985, *ApJ*, 295, 109  
 Müller, M., & Weigelt, G. 1987, *A&A*, 175, 312  
 Neri, R., & Grewing, M. 1988, *A&A*, 196, 338  
 Paresce, F. 1990, *Faint Object Camera Instrument Handbook, Version 2.0* (Baltimore: Space Telescope Science Institute)  
 Walborn, N. R. 1973, *ApJ*, 182, L21  
 ———. 1984, in *IAU Symp. 108, Structure and Evolution of the Magellanic Clouds*, ed. S. van den Bergh & K. S. de Boer (Dordrecht: Reidel), 243  
 ———. 1986, in *IAU Symp. 116, Luminous Stars and Associations in Galaxies*, ed. C. W. H. de Loore, A. J. Willis, & P. Laskarides (Dordrecht: Reidel), 185  
 ———. 1990, in *IAU Symp. 148, The Magellanic Clouds*, ed. R. Haynes & D. Milne (Dordrecht: Reidel), 145  
 Walborn, N. R., & Blades, J. C. 1987, *ApJ*, 323, L65  
 Walker, A. R., & O'Donoghue, D. E. 1984, *Astr. Express*, 1, 45  
 Weigelt, G., & Baier, G. 1985, *A&A*, 150, L18